ELSEVIER

International Journal of Heat and Fluid Flow 22 (2001) 102–110

International Journal of
HEAT AND FLUID FLOW

www.elsevier.com/locate/ijhff

Numerical investigation of forced convection heat transfer in porous media using a thermal non-equilibrium model

Pei-Xue Jiang *, Ze-Pei Ren

Department of Thermal Engineering, Tsinghua University, Beijing 100084, People's Republic of China

Received 3 September 1999; accepted 11 April 2000

Abstract

In the present paper, the effects of viscous dissipation, the boundary condition assumptions, thermal dispersion, particle diameters and the variable properties of oil on convection heat transfer are analyzed using a numerical model including thermal non-equilibrium assumption. The results, which are compared with experimental data, show that the convection heat transfer in porous media can be predicted numerically using the thermal non-equilibrium model with the ideal constant wall heat flux boundary condition. Viscous dissipation weakens the convection heat transfer from the fluid to the wall in the porous media. However, under practical conditions the influence of viscous dissipation on the convection heat transfer is small. The fluid temperature in the bottom part of the channel is higher than in the core region of the channel when the lower plate is adiabatic due to the effect of viscous dissipation. The variation of the thermal physical properties of oil has a profound influence on the convection heat transfer coefficient, which increases as the heat flux increases. When the upper and lower plates are heated with the same heat flux, the convection heat transfer coefficient on the upper plate surface is higher than when one side is heated and the other is insulated. However, the differences caused by these two kinds of boundary conditions in porous media are less than that in an empty channel.

Keywords: Porous media; Heat transfer; Viscous dissipation; Boundary condition; Thermal non-equilibrium; Thermal dispersion

1. Introduction

Convection heat transfer in porous media has been extensively investigated due to its many important engineering applications. From the point of view of the energy equation there are two different models in theoretical and numerical research: local thermal equilibrium model and local thermal non-equilibrium model. The local thermal equilibrium model assumes that the solid-phase temperature is equal to the fluid temperature, i.e., local thermal equilibrium between the fluid and the solid-phases at any location in the porous media. This model simplifies theoretical and numerical research, but the assumption of local thermal equilibrium between the fluid and the solid-phases is inadequate for a number of problems. Although the classical thermal non-equilibrium model (Schumann model) was presented 70 years ago, only in recent years more attention has been paid to the local thermal non-equilibrium model and its use has increased in theoretical and numerical research as deep-going understanding of the convection heat transfer processes in porous media. Representative works include Carbonnel and Whitaker (1984), Vafai and Sozen (1990), Quintard and Whitaker (1993), Quintard et al. (1997), Quintard (1998), Amiri and Vafai (1994), Amiri et al. (1995), Batsale et al. (1996), Jiang et al. (1996, 1999a), Kuznetsov (1997, 1998), Nield (1998), Hsieh and Lu (1998), Peterson and Chang (1998), Martin et al. (1998), Spiga and Morini (1999), and Lee and Vafai (1999), etc.

Quintard (1998) pointed out that when using two-equation (or two-temperature) models several questions need to be solved. For example, what is the relevance of this model with respect to the pore-scale physical problem? How are the macroscopic properties related to the pore-scale physical properties of the system? Many of these questions have been clarified in a series of articles during the last decade (Carbonnel and Whitaker, 1984; Quintard and Whitaker, 1993; Batsale et al., 1996; Quintard et al., 1997). Research has shown that the two-equation model cannot handle high-frequency heat waves. Several numerical experiments have been carried out to prove its usefulness (Quintard and Whitaker, 1993). A general two-temperature model dealing with local non-equilibrium heat transfer in porous media was presented by Quintard (1998) by adding the effect of interfacial thermal barriers and the heat exchange flux in the macroscopic equations was approximated as a time convolution integral involving the temperature at the boundary. However, the two-temperature model presented in Quintard (1998) is not easily implemented. Moreover, according to Quintard (1998), under some conditions (e.g., if the

* Corresponding author. Tel.: +86-10-62772661; fax: +86-10-62770209.
E-mail address: jiangpx@te.tsinghua.edu.cn (P.-X. Jiang).

0142-727X/01/$ - see front matter
PII: S 0 1 4 2 - 7 2 7 X (0 0) 0 0 0 6 6 - 7

Notation

a_f	fluid thermal diffusivity (m^2/s)
c_p	fluid specific heat (J/(kg K))
C^*	constant in Eq. (12) (dimensionless)
d_p	particle diameter (m)
D_e	equivalent diameter of the porous plate channel ($=2hW/(h+W)$) (m)
F	inertia coefficient (dimensionless)
G	mass flow rate (kg/s)
h	channel height (m)
h_f	fluid specific enthalpy (J/kg)
h_x	local heat transfer coefficient (W/m^2 K)
h_{sf}	heat transfer coefficient between solid particles and the fluid (W/m^2 K)
h_v	volumetric heat transfer coefficient between solid particles and the fluid (W/m^3 K)
K	permeability of porous medium (m^2)
L	channel length (m)
Nu_{sf}	Nusselt number for convection heat transfer between solid particles and the fluid (dimensionless)
p	pressure (Pa)
Pe	Peclet number ($=Re\,Pr$) (dimensionless)
Pr	Prandtl number (dimensionless)
q	heat flux (W/m^2)
Re	Reynolds number (dimensionless)
T	temperature (K)
u_p	pore velocity in the x-direction (m/s)
U_p	pore velocity ($=(u_p^2+v_p^2)^{1/2}$) (m/s)
$\lvert\vec{V}\rvert$	Darcian velocity ($=(u^2+v^2)^{1/2}$) (m/s)
v_p	pore velocity in the y-direction (m/s)
W	channel width (m)
x, y	coordinates in the flow region (m)

Greeks

λ	thermal conductivity (W/m K)
λ_d	dispersive component of thermal conductivity (W/m K)
λ_f	fluid thermal conductivity (W/m K)
λ_m	stagnant effective thermal conductivity of fluid and porous media (W/m K)
λ_s	solid particles thermal conductivity (W/m K)
μ	fluid absolute viscosity (N s/m^2)
μ_e	effective absolute viscosity ($\approx\mu_f$) (N s/m^2)
ρ	fluid density (kg/m^3)
ε	porosity (dimensionless)
ε_m	mean porosity (dimensionless)
ε_∞	porosity at channel center ($=\varepsilon_m/(1+0.567d_p/h(1-e^{-3h/d_p}))$) [dimensionless] (Jiang et al., 1999a)

Subscripts

b	bulk mean temperature
d	dispersion
f	fluid
p	pore
s	solid
0	heated section inlet
w	wall
1	upper wall
2	lower wall

frequency of the fluid-phase temperature variations is small enough so that a single heat wave enters the solid-phase) the time convolution integral for the heat exchange flux presented by Quintard (1998) can be approximated by the volumetric heat transfer coefficient multiplied by the temperature difference between the solid- and fluid-phases, which is the usual expression for the two-equation model. Most cases consider steady-state heat transfer processes, so that the usual two-equation model is used widely.

Vafai and Sozen (1990), Amiri and Vafai (1994) and Amiri et al. (1995) thoroughly investigated the forced convection heat transfer in porous media using the thermal non-equilibrium model. Their works analyzed the effects of non-Darcy flow, variable porosity, solid-to-fluid thermal diffusivity ratio and thermal dispersion. The effects of constant wall temperature and constant wall heat flux boundary conditions on the thermal response of the bed were discussed by Amiri et al. (1995). Jiang et al. (1996) used constant wall heat flux boundary conditions to investigate the effects of the local thermal non-equilibrium, the thermal conductivity of the solid particles and the particle diameter on the convection heat transfer. Jiang et al. (1999a) considered thermal dispersion effects in glass packed beds using both the local thermal equilibrium model and the local thermal non-equilibrium model and found that both numerical simulation results corresponded well with the experimental results. However, in the case of water in metallic porous media the numerical results using the local thermal non-equilibrium model with consideration of the thermal dispersion effect corresponded well with the experimental results, while the results predicted using the thermal equilibrium model were significantly different.

When using the thermal non-equilibrium model, the treatment of the boundary conditions of the energy equations is not an insignificant matter (Amiri et al., 1995). Reasonable assumptions for the boundary conditions are needed to obtain correct numerical results. A number of papers have concerned themselves with this problem, e.g. (Amiri et al., 1995; Jiang et al., 1996, 1999a; Hsieh and Lu, 1998; Martin et al., 1998; Lee and Vafai, 1999). For the case of constant wall heat flux there are four different assumptions or treatment methods for the boundary conditions of the energy equations. The main difference between them is whether the fluid temperature is equal to the solid-phase temperature on the wall. Amiri et al. (1995) and Jiang et al. (1996, 1999a) found that the numerical results assuming that the heat flux transferred by solid particles was equal to that transferred by the fluid on the wall for the constant wall heat flux boundary conditions agreed well with experimental data. However, Hsieh and Lu (1998), Peterson and Chang (1998), Martin et al. (1998) and Lee and Vafai (1999) assumed that the fluid temperature was equal to the solid-phase temperature on the wall for the constant heat flux boundary conditions. In the present paper, the reliability of the various treatments of the constant wall heat flux boundary conditions will be analyzed by comparing numerical simulation results with experimental data.

The effect of thermal dispersion on the forced convection heat transfer in porous media is another important topic. It is well known that the transverse thermal dispersion effect plays an important role on forced convection heat transfer in porous media. However, there are different viewpoints on the effect of longitudinal thermal dispersion on the convection heat transfer. Recently, Kuwahara and Nakayama (1999) numerically investigated the effect of the longitudinal thermal dispersion coefficient by considering a macroscopically uniform flow through a periodic model of square rods. The numerical results agree well with the experimental data obtained by Fried and Combarnous (1971) for the longitudinal dispersion coefficients in packed beds. The results showed that the longitudinal dispersion is substantially higher than the transverse dispersion. However, according to Kuo and Tien (1988), Hunt and Tien (1990), Hsu and Cheng (1990) and Sozen and Vafai (1993), the longitudinal thermal dispersion effects can be neglected without causing significant errors in the heat transfer results. The different conclusions may depend on whether the temperature gradient along the longitudinal direction is much less than the transverse temperature gradient in the porous channels when the heat is mainly transferred perpendicularly from the wall to the flowing fluid. In the present paper, the longitudinal diffusion and dispersion will be neglected. The present authors are currently undertaking a new investigation of the effect of the longitudinal thermal dispersion.

Similar models for transverse thermal dispersion were presented in Yagi et al. (1960), Wakao and Kaguei (1982), Hunt and Tien (1988), Kuo and Tien (1988), Hsu and Cheng (1990), Masuoka and Takatsu (1996) and Kuwahara et al. (1996). The coefficients presented in these models, however, vary by as much as thirty folds. Jiang et al. (1999a) used experimental data (Jiang et al., 1999b) to develop a modified thermal dispersion conductivity model in which the coefficient is not constant. This paper analyzes whether the decrease of the coefficient in the thermal dispersion conductivity model as the velocity increases is a result of viscous dissipation.

Bejan (1984) derived a model of viscous dissipation for Darcy flow in saturated porous media. Fand et al. (1986) experimentally investigated the free convection heat transfer from a horizontal cylinder embedded in a porous medium which is saturated by water or silicon oil. An appreciable change in the heat transfer rate was observed due to the viscous dissipation in the Darcy flow region with silicon oil as the saturated fluid. Murthy and Singh (1997, 1998) studied the effect of viscous dissipation on non-Darcy natural or mixed convection in porous media with and without the thermal dispersion effect. Their results showed that viscous dissipation caused a significant decrease in the heat transfer rate. It was also observed that the dissipation effect increased as the thermal dispersion parameter increased and the viscous dissipation decreased the heat transfer rate in both aiding and opposing flows. The effects of thermal dispersion and the effect of viscous dissipation on the heat transfer rate were studied using non-dimensional parameters (e.g., Gebhart number $Ge_x = g\beta x/c_p$) by Murthy and Singh (1997, 1998). However, the values of Ge_x used in Murthy and Singh (1997, 1998) are difficult to realize. For example, for $c_p = 1005$ J/kg K and $\beta = 3 \times 10^{-3}$ K^{-1}, $Ge_x = 0.1$ means $x = 3418$ m! In addition, only the local thermal equilibrium model was used in Fand et al. (1986) and Murthy and Singh (1997, 1998).

The present paper investigates the effects of viscous dissipation, appropriate boundary conditions, thermal dispersion, particle diameters and the variable properties of oil on the convection heat transfer in porous media using numerical model including thermal non-equilibrium. The numerical results are compared with experimental data.

2. Theoretical analysis and physical–mathematical model

In order to compare the numerical results with the experimental data in Jiang et al. (1999b), the physical model in the present paper is similar to the test section in Jiang et al. (1999b). The physical model and the coordinate system are shown in Fig. 1. The analysis assumes that the porous media is homogeneous and isotropic. The upper plate of the channel receives a constant heat flux, q_{w1}, while the lower plate is either adiabatic or heated with a constant heat flux, q_{w2} . An adiabatic section was placed before the heated section. Fluid flow entered the channel with a uniform velocity, u_0, and constant

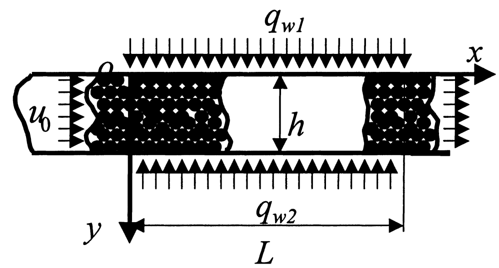

Fig. 1. Schematic diagram of the physical system.

temperature, T_{f0}. The fluid flow is single-phase and two-dimensional, steady, and non-Darcian. The longitudinal conduction in the fluid and the pressure variation in the y-direction are assumed to be negligible according to Kuo and Tien (1988), Hsu and Cheng (1990), Sozen and Vafai (1993), etc.

The steady-state, two-dimensional governing equations for single-phase fluid flow in an isotropic, homogeneous porous medium based on the Brinkman–Darcy–Forchheimer model with consideration of variable properties and variable porosity can be written in the following form:

$$\frac{\partial(\rho_f \varepsilon u_p)}{\partial x} + \frac{\partial(\rho_f \varepsilon v_p)}{\partial y} = 0, \tag{1}$$

$$\frac{\partial(\rho_f \varepsilon u_p u_p)}{\partial x} + \frac{\partial(\rho_f \varepsilon v_p u_p)}{\partial y} = -\frac{\partial(\varepsilon p)}{\partial x} - \varepsilon^2 \frac{\mu_f}{K} u_p - \varepsilon^3 \frac{\rho_f F}{\sqrt{K}} |U_p| u_p + \frac{\partial}{\partial y}\left(\varepsilon \mu_e \frac{\partial u_p}{\partial y}\right), \tag{2}$$

$$\int_0^h \rho_f \varepsilon u_p \, dy = \rho_0 u_0 h. \tag{3}$$

The corresponding velocity boundary conditions are:

$$y = 0, \quad u_p = v_p = 0,$$
$$y = h, \quad u_p = v_p = 0.$$

The energy equations for the fluid- and solid-phases using the thermal non-equilibrium model with longitudinal thermal conduction in the solid-phase and without viscous dissipation were presented in Jiang et al. (1999a). The mechanism of viscous dissipation is the conversion of work required to sustain the motion of a real fluid into heat by the action of viscosity. In porous media, the contact surface between the fluid and the solid particles is very large, so the work required to sustain the fluid motion increases dramatically. Therefore, the effect of viscous dissipation increases. Bejan (1984) pointed out that the dissipation term in porous media equals the mechanical power needed to extrude the viscous fluid through the pore. According to Bejan (1984), Fand et al. (1986) and Murthy and Singh (1997, 1998), the fluid-phase and solid-phase energy equations with consideration of thermal dispersion, viscous dissipation, variable porosity and variable properties, while neglecting the longitudinal thermal conduction of the solid particles, are:

$$\frac{\partial(\rho_f \varepsilon u_p h_f)}{\partial x} + \frac{\partial(\rho_f \varepsilon v_p h_f)}{\partial y} = \frac{\partial}{\partial y}\left[\frac{\lambda_f \varepsilon + \lambda_d}{c_{p_f}} \frac{\partial h_f}{\partial y}\right] + \frac{\varepsilon^2 \mu_f}{K} u_p^2 + \frac{\varepsilon^3 \rho_f F}{\sqrt{K}} |U_p| u_p^2 + h_v (T_s - T_f), \tag{4}$$

$$\frac{\partial}{\partial y}\left[\lambda_s(1-\varepsilon)\frac{\partial T_s}{\partial y}\right] - h_v(T_s - T_f) = 0. \tag{5}$$

There are four different methods for treating the boundary conditions for the energy equations in the case of constant wall heat flux:

- Amiri et al. (1995) and Jiang et al. (1996, 1999a)

$$q_w = -\lambda_{fw}(\partial T_f/\partial y)_w = -\lambda_s(\partial T_s/\partial y)_w. \tag{6}$$

- Martin et al. (1998)

$$q_w = -(\varepsilon\lambda_f + (1-\varepsilon)\lambda_s)_w(\partial T/\partial y)_w, \quad T_{ws} = T_{wf}. \tag{7}$$

- Lee and Vafai (1999)

$$q_w = -\varepsilon_w\lambda_{fw}(\partial T_f/\partial y)_w - (1-\varepsilon_w)\lambda_s(\partial T_s/\partial y)_w,$$
$$T_{ws} = T_{wf}. \tag{8}$$

The other possible method is

$$q_w = -\lambda_m(\partial T/\partial y)_w, \quad T_{ws} = T_{wf}. \tag{9}$$

The parameters used in Eqs. (1)–(9) were obtained from Dixon and Cresswell (1979),Vafai (1984), Hunt and Tien (1988), Hsu and Cheng (1990) and Achenbach (1995).

$$K = d_p^2\varepsilon^3\Big/\left(150(1-\varepsilon)^2\right), \quad F = 1.75\Big/\left(\sqrt{150}\varepsilon^{3/2}\right),$$

$$\varepsilon = \varepsilon_\infty\left(1 + 1.7e^{-6y/d_p}\right) \quad (0 \leqslant y \leqslant h/2),$$

$$\varepsilon = \varepsilon_\infty\left(1 + 1.7e^{-6(h-y)/d_p}\right) \quad (h/2 \leqslant y \leqslant h),$$

$$\frac{\lambda_m}{\lambda_f} = [1 - \sqrt{1-\varepsilon}] + \frac{2\sqrt{1-\varepsilon}}{1-\sigma B}\left[\frac{(1-\sigma)B}{(1-\sigma B)^2}\ln\left(\frac{1}{\sigma B}\right) - \frac{B+1}{2} - \frac{B-1}{1-\sigma B}\right], \tag{10}$$

$$B = 1.25((1-\varepsilon)/\varepsilon)^{10/9}, \quad \sigma = \lambda_f/\lambda_s, \quad h_v = h_{sf}\cdot 6(1-\varepsilon)/d_p,$$

$$Nu_{sf} = h_{sf}d_p\lambda_f = \left[\left(1.18Re^{0.58}\right)^4 + \left(0.23Re_h^{0.75}\right)^4\right]^{1/4},$$

(Achenbach, 1995),

$$\frac{1}{h_{sf}} = \frac{d_p}{Nu_{sf}\lambda_f} + \frac{d_p}{\beta\lambda_s},$$

$$Nu_{sf} = \frac{0.255}{\varepsilon}Pr^{1/3}Re^{2/3}, \quad \beta = 10,$$

(Dixon and Cresswell, 1979),

$$Re = \varepsilon\rho u_p d_p/\mu, \quad Re_h = Re/(1-\varepsilon).$$

For $Re \gg 10$, Hsu and Cheng (1990) presented the following thermal dispersion conductivity model:

$$\lambda_d = 0.04\lambda_f\frac{1-\varepsilon}{\varepsilon}\frac{|\vec{V}|d_p}{a_f} = 0.04\lambda_f\frac{1-\varepsilon}{\varepsilon}Pe. \tag{11}$$

For $Re \ll 10$, the thermal dispersion conductivity can be calculated according to Hsu and Cheng (1990):

$$\lambda_d = C^*\lambda_f\frac{1-\varepsilon}{\varepsilon^2}\frac{|\vec{V}|^2d_p^2}{a_f^2} = C^*\lambda_f\frac{1-\varepsilon}{\varepsilon^2}Pe^2. \tag{12}$$

Jiang et al. (1999a) presented the following modified thermal dispersion conductivity model for water in porous media:

$$\lambda_d = C(\rho c_p)_f d_p\sqrt{u_p^2 + vp^2}(1-\varepsilon),$$
$$C = 1.042(\rho_f c_{pf} d_p u_p(1-\varepsilon_m))_0^{-0.8282}. \tag{13}$$

where, the coefficient C is a dimensionless value but is a function of the value of $[\rho_f c_{pf} d_p u_p(1-\varepsilon_m)]_0$ when all of the parameters use standard metric units. Eq. (13) corresponds well to the different thermal dispersion models that use various constants for different cases. The numerical simulation results using Eq. (13) correspond well to the experimental data (Jiang et al., 1999a). Therefore, Eq. (13) is a more comprehensive model than the usual thermal dispersion model with constant C.

3. Numerical method

The governing equations were solved numerically using the finite difference method. Using the appropriate dimensionless parameters, Eqs. (1)–(5) and the boundary conditions were first transformed into dimensionless form. Then the dimensionless governing equations were discretized using control volume integration. The governing equations are parabolic in the x-direction. Therefore, Eqs. (1)–(5) can be solved by marching in the downstream direction. A similar numerical method can be found in Jiang et al. (1996). The no-slip boundary conditions and the variable porosity resulted in steep velocity gradients near the wall. Calculations with various numbers of elements (e.g., $202\times 52, 202\times 102$, and 202×202) showed that for an adequate grid point distribution, the numerical results do not depend on the number of grid points. Therefore, a non-uniform grid was employed with 102 grid points normal to the wall and 202 grid points in the axial direction. The property values used in the calculations were determined by second-order interpolation relative to enthalpy.

The local heat transfer coefficient on the upper wall was evaluated as

$$h_x = \frac{q_w}{T_{fw}(x) - T_{fb}(x)}. \tag{14}$$

4. Results and discussion

The size of the porous plate channel was $L = 58$ mm, $h = 5$ mm, and $W = 80$ mm. The numerical simulation used three different particle materials: glass beads, stainless steel and bronze. The thermal conductivities of these materials are 0.744, 16.4 and 75.35 W/m K, respectively. The particle diameters in the numerical calculations were 0.5, 0.428, 0.1 and 0.05 mm.

The numerical results were checked in numerous ways to verify the reliability of the physical–mathematical model, the solution procedures and the numerical simulation program. A detailed description of the simulation verification can be found in Jiang et al. (1999a). The velocity profiles and the fully developed temperature profile are compared with the analytical solution of Vafai and Kim (1989, 1995) in that paper, along with a comparison of the friction factors predicted by the numerical calculation and measured experimentally.

4.1. Effect of boundary condition method on the calculated convection heat transfer

The thermal non-equilibrium model was used with the different boundary condition methods (Eqs. (6)–(9)) and the thermal dispersion conductivity calculated by Eq. (13) to numerically predict the local convection heat transfer coefficients in a porous plate channel filled with glass or bronze particles.

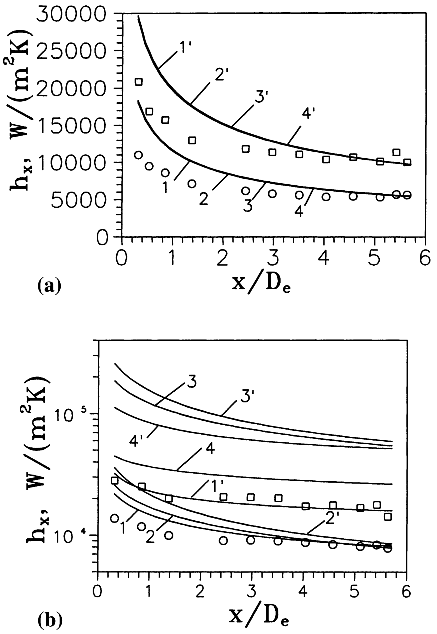

Fig. 2. Comparison of measured convection heat transfer coefficients with numerically simulated values for different boundary condition assumptions: (a) water–glass packed bed, $d_p = 0.428$ mm, $\varepsilon_m = 0.366$, $\lambda_s = 0.744$ W/m K; 1, 2, 3, 4, (○) $G = 0.03455$ kg/s; 1′, 2′, 3′, 4′, (□) $G = 0.1108$ kg/s; (b) water–bronze packed bed, $d_p = 0.428$ mm, $\varepsilon_m = 0.365$, $\lambda_s = 75.35$ W/m K; 1, 2, 3, 4, (○) $G = 0.0542$ kg/s; 1′, 2′, 3′, 4′, (□) $G = 0.1266$ kg/s. Assumptions of boundary condition: curves 1 and 1′ used Eq. (6); 2, 2′ – Eq. (9); 3, 3′ – Eq. (7); 4, 4′ – Eq. (8); (○, □) experimental data in Jiang et al. (1999b).

Comparison of the results with the experimental data in Jiang et al. (1999b), Fig. 2(a), shows that for the glass bead bed the numerical simulation results for all four boundary condition methods (Eqs. (6)–(9)) are very close and correspond well to the experimental results if the larger experimental errors in the inlet section are taken into account. The results are essentially the same because the thermal conductivities of water and the glass beads are very similar; therefore, the fluid and the solid-phases are very near local thermal equilibrium at any location in the porous media. The different assumptions for the energy equation boundary conditions have little influence on the numerical results.

For the porous plate channel filled with bronze particles, Fig. 2(b), use of the constant wall heat flux assumption for the boundary conditions, Eq. (6), results in simulation results that correspond well to the experimental data. When the energy equation boundary conditions given in Eq. (7) is used, the numerical results are much higher than the experimental data, because Eq. (7) over predicts the effective thermal conductivity (e.g., for $\varepsilon_w = 0.94$, $\lambda_s = 75.35$ W/m K, $\lambda_f = 0.6$ W/m K, $(\varepsilon\lambda_f + (1-\varepsilon)\lambda_s)_w = 5.09$ W/m K). However, when the energy equation boundary conditions given in Eq. (9) is used, the numerical results are lower than the experimental data, because the effective thermal conductivity calculated by Eq. (10) is too small (e.g., for $\varepsilon_w = 0.94$, $\lambda_s = 75.35$ W/m K, $\lambda_f = 0.6$ W/m K, $\lambda_m = 0.7$ W/m K according to Eq. (10)). At the present time, the conditions given in Eq. (8) are the most popular method for treating the constant heat flux boundary condition, as shown in Hsieh and Lu (1998), Peterson and Chang (1998), Martin et al. (1998) and Lee and Vafai (1999). Hsieh and Lu (1998) used Eq. (8) for the heating surface boundary condition, but used $(\partial T_f/\partial y)_w = (\partial T_s/\partial y)_w = 0$ for the adiabatic surface. Therefore, the fluid temperature and the solid particle temperature at the adiabatic wall are not equal, which contradicts their assumption that at the wall the solid particle temperature is equal to the fluid temperature. The theoretical basis for Eq. (8) is that the actual heated wall in the experiments has a finite thickness and the fluid temperature and solid particle temperature at adjacent locations on the wall are equal due to the thermal conduction in the wall. The heat flux from the wall is then transferred concurrently by the fluid- and the solid-phase. Therefore, regardless of whether $q_{w1} \neq 0$ or $q_{w2} = 0$, Eq. (8) should result in equal fluid- and solid-phase temperatures at the wall. The boundary condition treatment used by Hsieh and Lu (1998) is a mixture of Eq. (6) and (8). However, with the boundary conditions given by Eq. (8), the numerical results in this paper are much higher than the experimental data, Fig. 2(b).

From a completely rigorous point of view, for constant wall heat flux boundary conditions in the experiments with finite wall thickness, the heat fluxes transferred by the fluid and the solid-phases at adjacent locations are unequal. The fluid and the solid-phase temperatures at adjacent locations are also unequal. Therefore, the condition given in Eq. (8) implies that the local thermal equilibrium condition is imposed on all locations on the wall. Kenning and Yan (1995) investigated pool boiling of water in an open tank with an immersed thin (0.13 mm thick), electrically heated stainless steel plate using liquid–crystal thermography in combination with high-speed video recording. They found that for the constant wall heat flux boundary condition, the heated wall temperature at the nucleation sites differed from the heated wall temperature of the surrounding regions. The measurements confirmed the importance of variations in wall temperature for the removal of heat by bubbles and the activity of nucleation sites. Kenning and Yan (1995) concluded that models in which uniform wall temperature is assumed cannot represent the fundamental physics of boiling. Their results have some implications for our problem. For very thin heated walls, the fluid- and solid-phase temperatures at the wall will differ for porous media with large thermal conductivity difference between the fluid and the solid particles.

Laminar convection heat transfer in tubes or channels with the constant wall heat flux boundary condition differs from that with the constant wall temperature boundary condition. Although the wall temperature difference, ΔT_w, at a small longitudinal step Δx, may be small, ΔT_w is not zero. Since $\Delta T_w = 0$ will lead to $T_w =$ constant. Therefore, although the difference between the fluid and solid particle temperatures at the wall in porous media may be small, $T_{ws} = T_{wf}$ as given in Eqs. (7)–(9) may not be reliable.

Eq. (6) assumes that the heat fluxes transferred separately by the fluid and the solid-phases are equal to the wall heat flux. When the heated wall is very thin, this assumption may be reasonable and might be considered as an ideal boundary condition. In experimental research, the constant wall heat flux boundary condition is often realized using electrical heating. The fluid temperature may be very close to the solid particle temperature at the wall due to thermal conduction in the wall, so the experimental boundary conditions differ from the ideal boundary conditions given in Eq. (6). However, comparison of the simulation results using the boundary conditions in Eq. (6) with the experimental results shows that the convection heat transfer in porous media can be predicted numerically using the ideal boundary conditions (Eq. (6)). This conclusion should be further verified by comparing numerical results with more experimental data. The rest of this paper uses the boundary conditions given in Eq. (6). The thermal dispersion conductivity will be calculated using Eq. (13) if not otherwise stated.

4.2. Effect of viscous dissipation on convection heat transfer in porous media

Jiang et al. (1999a) found that the coefficient in the thermal dispersion conductivity model decreases as the velocity increases (Eq. (13)). In porous media, the contact surface between the fluid and the solid particles is very large; therefore, the effect of viscous dissipation increases. This invites the question of whether the decrease of the coefficient in the thermal dispersion conductivity model, Eq. (13), can be ascribed to viscous dissipation? The experimental results in Jiang et al. (1999b) are compared with the simulation results for convection heat transfer in water with stainless steel or bronze porous media with or without consideration of viscous dissipation in Fig. 3. The results show that the effect of viscous dissipation is negligible for the given conditions. The numerical results with the thermal dispersion conductivity calculated using Eq. (13) correspond well to the experimental results. However, the numerical results with the thermal dispersion conductivity calculated using Eq. (11) are much higher than the experimental results, while the influence of viscous dissipation is also very small. Therefore, the decrease of the coefficient in the thermal dispersion conductivity model, Eq. (13), was not caused by viscous dissipation.

It is shown from the energy equation, Eq. (4), that the effect of viscous dissipation increases as the velocity or viscosity increases or the particle diameter decreases. The effect of viscous dissipation on the heat transfer rate was studied by Murthy and Singh (1997, 1998) using the non-dimensional Gebhart number, $Ge_x = g\beta x/c_p$. However, $Ge_x = 0.1$ in Murthy and Singh (1997, 1998) is impractical (as mentioned above, for $c_p = 1005$ J/kg K and $\beta = 3 \times 10^{-3}$ K^{-1}, $Ge_x = 0.1$ means $x = 3418$ m!). The present paper studies the effect of viscous dissipation for more practical values of the dimensional parameters.

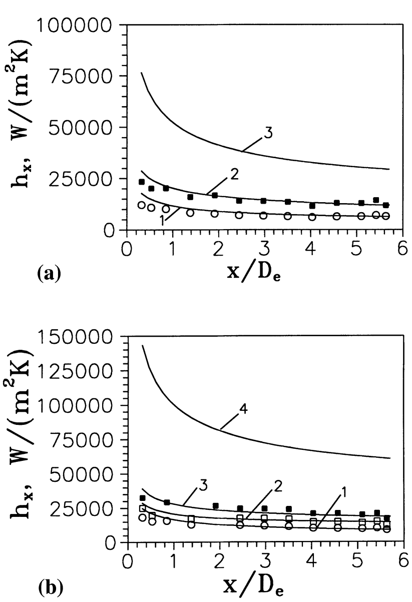

Fig. 3. Numerically simulated local heat transfer coefficients with (——) or without (– – –) consideration of viscous dissipation and measured data for (a) stainless steel or (b) bronze packed beds. (○, □, ■) experimental data in Jiang et al. (1999b); $d_p = 0.428$ mm; $\varepsilon_m = 0.365$; $q_{w2} = 0$; (a) G (kg/s); 1, (○) 0.031; 2, 3, (■) 0.1006; λ_d: 1, 2 – Eq. (13); 3 – Eq. (11); (b) G (kg/s): 1, (○) 0.0721; 2, (□) 0.0973; 3, 4, (■) 0.1964; λ_d: 1, 2, 3 – Eq. (13); 4 – Eq. (11).

The influence of viscous dissipation on the convection heat transfer in water with glass beads or bronze particles with small particle diameters and high velocities is presented in Fig. 4. The physical model is identical to that of the test section in Jiang et al. (1999b), i.e., $L = 58$ mm, $h = 5$ mm, and $W = 80$ mm. For $\rho u = 1250$ kg/m^2 s the pressure drop for $d_p = 0.1$ mm is 31 MPa and that for $d_p = 0.05$ mm is 80 MPa. This is an extreme condition which is difficult to realize, but even for such conditions, the influence of viscous dissipation on the convection heat transfer of water in porous media is small (<0.3%). In addition, the results in Fig. 4(a) shows that for the glass beads porous channel with water as the working fluid, the convection heat transfer coefficient increases as the particle diameter increases; whereas for the bronze particles porous channel with water as the working fluid, the convection heat transfer coefficient increases as the particle diameter decreases (Fig. 4(b)). These results are identical to previous research by Jiang et al. (1996, 1999b). The opposing trends result from the competing factors of the mixing effects (or thermal dispersion) and the decreased contact surface area between particles as the particle diameter increases. Detailed analysis of the effect of particle diameter on the convection heat transfer can be found in Jiang et al. (1996, 1999b). A criterion for judging the variation of the convection heat transfer coefficient with d_p was presented in Jiang et al. (1999b).

In order to further study the effect of viscous dissipation, the present paper considers the convection heat transfer for lubrication oil (No. 14) in porous media. The Reynolds number based on the particle diameter, Re, may be less than 10 due to the high viscosity of the oil. The thermal dispersion conductivity should be calculated using Eq. (12) according to Hsu and Cheng (1990); however, the value of the coefficient C^* in Eq. (12) was not given in Hsu and Cheng (1990). The numerical results for the convection heat transfer of lubrication oil in glass porous media with consideration of thermal dispersion for $C^* = 10^{-7}$ or 10^{-8} are presented in Fig. 5. The numerically predicted convection heat transfer coefficients of lubrication oil in porous media without consideration of

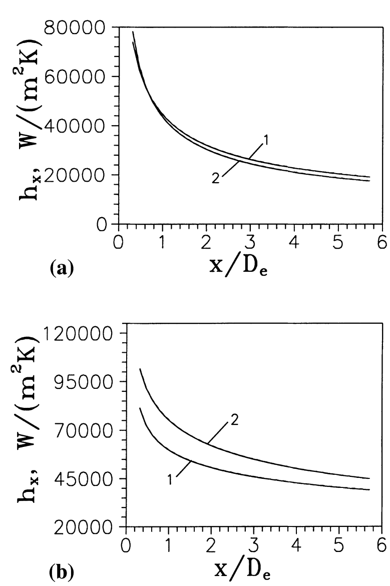

Fig. 4. Effects of viscous dissipation and particle diameter on the local heat transfer coefficient: (a) water–glass beads; (b) water–bronze particles (——) with viscous dissipation; (– – –) without viscous dissipation; $1 - d_p = 0.1$ mm; $\rho u = 1250$ kg/m^2 s; $\varepsilon_m = 0.366$; $q_{w1} = 7.71 \times 10^4$ W/m^2; $q_{w2} = 0$; $2 - d_p = 0.05$ mm; $\rho u = 1250$ kg/m^2 s; $\varepsilon_m = 0.366$; $q_{w1} = 1 \times 10^5$ W/m^2; $q_{w2} = 0$.

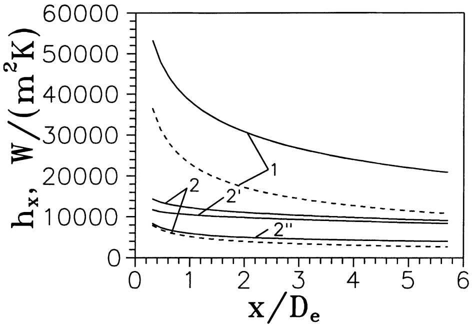

Fig. 5. Effect of thermal dispersion on heat transfer in porous media $d_p = 0.5$ mm, $\varepsilon_m = 0.366$, $\rho u = 1250$ kg/m^2 s; 1 – water–glass beads; $2, 2', 2''$ – lubrication oil – glass beads; (– – –) without consideration of thermal dispersion; (——) with consideration of thermal dispersion; 1, 2 – λ_d using model in Eq. (13); $2'$ – λ_d using Cheng's model, Eq. (12) with $C^* = 10^{-7}$ and $2''$ – λ_d using Cheng's model, Eq. (12) with $C^* = 10^{-8}$.

thermal dispersion or with consideration of thermal dispersion calculated using Eq. (13) are also presented in this figure. As a reference, the numerical results for convection heat transfer of water in porous media are also presented in Fig. 5. As shown in Fig. 5, the thermal dispersion significantly affects the convection heat transfer. The numerical results using Eq. (13) are close to those predicted using Eq. (12) with $C^* = 10^{-7}$. As the value of the coefficient C^* in Eq. (12) was not verified experimentally, the thermal dispersion conductivity in the following calculation will still use Eq. (13).

The numerically predicted convection heat transfer coefficients of lubrication oil in glass (Fig. 6(a)) or bronze (Fig. 6(b)) porous media with and without consideration of viscous dissipation are presented in Fig. 6. For the same physical region used earlier, when $\rho u = 1250$ kg/m^2 s and $d_p = 0.1$ mm the pressure drop is 3691 MPa. For such conditions, the viscous dissipation has some influence on the convection heat transfer (<2.2%). As mentioned by Murthy and Singh (1997, 1998), viscous dissipation reduces the convection heat transfer from the fluid to the wall in porous media. The results in Fig. 6 again show that the convection heat transfer coefficient increases as the particle diameter decreases when the thermal conductivity of the fluid is much less than the thermal conductivity of the solid particles. Comparing Fig. 6(a) with (b) shows that the convection heat transfer coefficients for lubrication oil in bronze packed beds are slightly higher than for lubrication oil in glass packed beds for the same conditions, but the differences are small. The results are similar because the lubrication oil viscosity is very large while the thermal conductivity is small (much less than the thermal conductivity of the particles). For, $T_f = 20$°C, $d_p = 0.5$ mm and $\rho u = 1250$ kg/m^2 s the Reynolds number is very small ($Re_{d_p} = 1.7$). As a result, the convection heat transfer between the lubrication oil and particles and the wall in porous media is fairly low and is the main thermal resistance, which dominates the overall heat transfer coefficient. Therefore, the effect of different solid particles on the overall heat transfer coefficient is not strong.

Fig. 7 presents the temperature distribution for lubrication oil in a glass bead bed with and without consideration of viscous dissipation. The fluid temperature with viscous dissipation is higher than the fluid temperature without viscous dissipation. For the conditions in Fig. 7, the maximum difference between them is 0.1°C. The fluid temperature on the bottom part of the channel is higher than in the core region of the channel when the lower plate is adiabatic due to the effect of viscous dissipation because the heat from the viscous dissipation heats the fluid on the bottom part of the channel. The

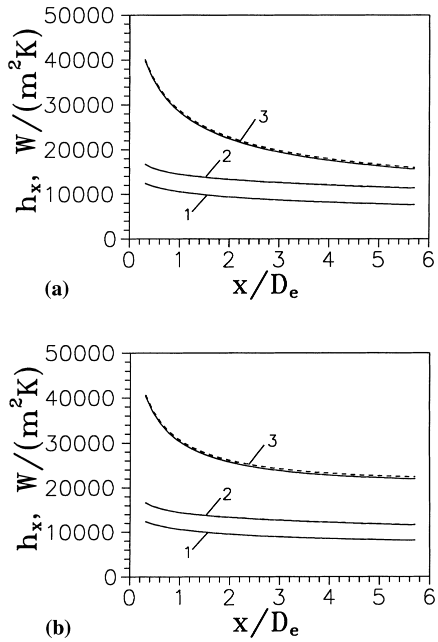

Fig. 6. Effects of viscous dissipation and particle diameter on the local heat transfer coefficient: (a) lubrication oil–glass beads; (b) lubrication oil – bronze particles (——) with consideration of viscous dissipation; (– – –) without consideration of viscous dissipation; $q_{w1} = 1 \times 10^5$ W/m^2; $q_{w2} = 0$; $\varepsilon_m = 0.366$; $1 - d_p = 0.5$ mm; $\rho u = 250$ kg/m^2 s; $2 - d_p = 0.5$ mm; $\rho u = 1250$ kg/m^2 s; $3 - d_p = 0.1$ mm; $\rho u = 1250$ kg/m^2 s .

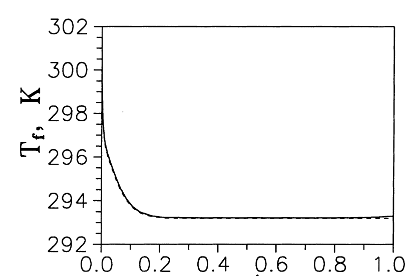

Fig. 7. Temperature distribution in lubrication oil with and without consideration of viscous dissipation in glass beads porous media at $x/D_e = 5.99$; $d_p = 0.5$ mm, $\rho u = 1250$ kg/m^2 s, $q_{w1} = 10^5$ W/m^2, $q_{w2} = 0$; (——) with viscous dissipation effect; (– – –) without viscous dissipation effect.

viscous dissipation plays a role analogous to an internal heat source.

4.3. Effect of variable properties of oil and heat flux on convection heat transfer

The thermal physical properties of oil vary sharply with temperature. The influence of the heat flux from the upper plate surface on the local convection heat transfer coefficient is presented in Fig. 8 with consideration of the variable physical properties. The variation of the thermal physical properties of oil has a profound influence on the convection heat transfer coefficient, which increases as the heat flux increases since the viscosity of the oil decreases sharply as the temperature rises, consequently intensifying the convection. At the same time, with increasing temperature the oil specific heat increases

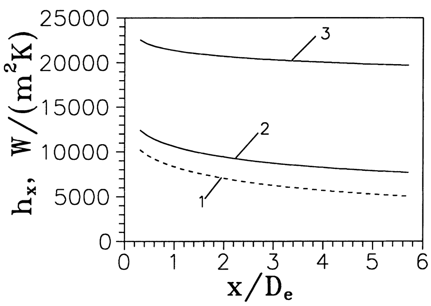

Fig. 8. Effect of variable physical properties of lubrication oil on heat transfer in porous media (lubrication oil–glass beads); $d_p = 0.5$ mm, $\rho u = 1250\,\mathrm{kg/m^2\,s}, \varepsilon_m = 0.366, q_{w2} = 0$; 1 – constant properties; 2 – variable properties, $q_{w1} = 10^5\,\mathrm{W/m^2}$; 3 – variable properties, $q_{w1} = 10^6\,\mathrm{W/m^2}$.

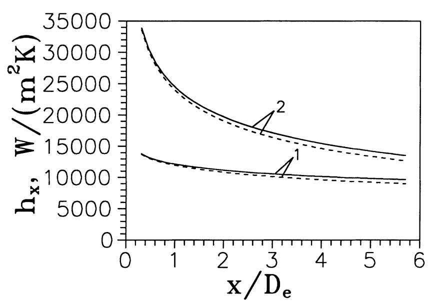

Fig. 9. Effect of wall heat flux on heat transfer coefficients: $d_p = 0.5$ mm, $\rho u = 500$ kg/m^2 s, $\varepsilon_m = 0.366$; 1 – lubrication oil–glass beads; 2 – water–glass beads; (– – –) $q_{w1} = 10^5\,\mathrm{W/m^2}$, $q_{w2} = 0$; (——) $q_{w1} = q_{w2} = 10^5\,\mathrm{W/m^2}$.

slightly, although the thermal conductivity and the oil density decrease a little. Therefore, the variation of the thermal physical properties of oil must be included in numerical and experimental research.

The influence of the heat flux from the lower plate surface on the convection heat transfer at the upper plate surface is presented in Fig. 9. The convection heat transfer coefficient on the upper plate surface when the upper and the lower plates have the same heat flux is higher than that when one side is heated and the other is adiabatic. However, the difference between them is smaller than the difference which occurs in an empty channel (without porous media). Kays and Crawford (1993) found that for fully developed laminar flow the convection heat transfer coefficient on the heated plate surface when both plates have the same heat flux is 52.9% larger than when one side is heated and the other is adiabatic. The difference decreases as the Reynolds number increases. As shown in Fig. 9, the convection heat transfer on the heated surface in porous media mainly depends on the flow and heat transfer conditions in the near wall region due to the intensive mixing of the fluid in the porous media. The influence of the flow and heat transfer conditions near the other wall region is weaker than in the case of the empty channel.

5. Conclusion

(1) The present paper numerically studies the influence of various assumptions for the energy equation boundary conditions in the thermal non-equilibrium model on the numerically predicted convection heat transfer by comparing with experimental data. The convection heat transfer coefficients in porous media predicted using the thermal non-equilibrium model with the ideal constant wall heat flux boundary condition (Eq. (6)) presented by Amiri et al. (1995) and Jiang et al. (1996, 1999a) are shown to correspond well to the experimental results for both high-thermal conductivity and low thermal conductivity porous media.

(2) The effect of viscous dissipation on the convection heat transfer in porous media is investigated numerically using the thermal non-equilibrium model. Viscous dissipation reduces the convection heat transfer on the wall in porous media. However, for most practical conditions viscous dissipation has little influence on the convection heat transfer. The fluid temperature when viscous dissipation is considered is higher than the fluid temperature without consideration of viscous dissipation. The fluid temperature on the bottom part of the channel is higher than in the core region of the channel when the lower plate is adiabatic due to the effect of viscous dissipation.

(3) The variation of the thermal physical properties of oil has a profound influence on the convection heat transfer coefficient, which increases as the heat flux increases.

(4) The convection heat transfer coefficient on the upper plate surface when the upper and lower plates with the same heat flux is higher than that when one side is heated and the other is adiabatic. However, the difference between them is smaller than for an empty channel (without porous media).

References

Achenbach, E., 1995. Heat and flow characteristics of packed beds. Experimental Thermal and Fluid Science 10, 17–27.

Amiri, A., Vafai, K., 1994. Analysis of dispersion effects and non-thermal equilibrium, non-Darcian, variable porosity incompressible flow through porous media. International Journal of Heat and Mass Transfer 37, 939–954.

Amiri, A., Vafai, K., Kuzay, T.M., 1995. Effects of boundary conditions on non-Darcian heat transfer through porous media and experimental comparisons. Numerical Heat Transfer (Part A) 27, 651–664.

Batsale, J., Gobbe, C., Quintard, M., 1996. Local non-equilibrium heat transfer in porous media. Recent Research Development in Heat, Mass and Momentum Transfer 1, Research Signpost, India, pp. 1–24.

Bejan, A., 1984. Convection Heat Transfer. Wiley.

Carbonnel, R.G., Whitaker, S., 1984. Heat and mass transfer in porous media. In: Bear, J., Corapcioglu, M.Y. (Eds.), Fundamentals of Transport Phenomena in Porous Media. Martinus Nijhoff, Dordrecht (Boston), pp. 121–198.

Dixon, A.G., Cresswell, D.L., 1979. Theoretical prediction of effective heat transfer parameters in packed beds. AIChE Journal 25, 663–676.

Fand, A.M., Steinberger, T.E., Cheng, P., 1986. Natural convection heat transfer from a horizontal cylinder embedded in porous media. International Journal of Heat and Mass Transfer 29, 119–133.

Fried, J.J., Combarnous, M.A., 1971. Dispersion in porous media. Advances in Hydroscience 7, 169–282.

Hsieh, W.H., Lu, S.F., 1998. Heat transfer analysis of thermally-developing region of annular porous media. In: Heat Transfer 1998, Proceedings of the 11th International Heat Transfer Conference, vol. 4, Kyongju, Korea, pp. 447–452.

Hsu, C.T., Cheng, P., 1990. Thermal dispersion in a porous medium. International Journal of Heat and Mass Transfer 33, 1587–1597.

Hunt, M.L., Tien, C.L., 1988. Non-Darcy convection in cylindrical packed beds. Journal of Heat Transfer 110, 378–384.

Hunt, M.L., Tien, C.L., 1990. Non-Darcian flow, heat and mass transfer in catalytic packed-bed reactors. Chemical Engineering Science 45, 55–63.

Jiang, P.X., Ren, Z.P., Wang, B.X., Wang, Z., 1996. Forced convective heat transfer in a plate channel filled with solid particles. Journal of Thermal Science 5, 43–53.

Jiang, P.X., Ren, Z.P., Wang, B.X., 1999a. Numerical simulation of forced convection heat transfer in porous plate channels using thermal equilibrium or non-thermal equilibrium models. Numerical Heat Transfer (Part A) 35, 99–113.

Jiang, P.X., Wang, Z., Ren, Z.P., 1999b. Experimental research of forced convection heat transfer in plate channel filled with glass or metallic particles. Experimental Thermal and Fluid Science 20, 45–54.

Kays, W.M., Crawford, M.E., 1993. Convective Heat and Mass Transfer, third ed. McGraw-Hill, New York.

Kenning, D.B.R., Yan, Y.Y., 1995. Pool boiling heat transfer on a thin plate: features revealed by liquid crystal thermography. Report of University of Oxford, No. OUEL 2055/95.

Kuo, S.M., Tien, C.L., 1988. Transverse dispersion in packed sphere bed. In: Proceedings of the 25th ASME Heat Transfer Conference, Houston, Texas, pp. 629–634.

Kuwahara, F., Nakayama, A., Koyama, H., 1996. A numerical study of thermal dispersion in porous media. Journal of Heat Transfer 118, 756–761.

Kuwahara, F., Nakayama, A., 1999. Numerical determination of thermal dispersion coefficients using a periodic porous structure. Journal of Heat Transfer 121, 160–163.

Kuznetsov, A.V., 1997. A perturbation solution for heating a rectangular sensible heat storage packed bed with a constant temperature at the walls. International Journal of Heat and Mass Transfer 40, 1001–1006.

Kuznetsov, A.V., 1998. Thermal non-equilibrium forced convection in porous media. In: Ingham, D.B., Pop, I. (Eds.), Transport Phenomena in Porous Media. Elsevier, Oxford, pp. 103–129.

Lee, D.Y., Vafai, K., 1999. Analytical characterization and conceptual assessment of solid and fluid temperature differences in porous media. International Journal of Heat and Mass Transfer 42, 423–435.

Martin, A.R., Saltiel, C., Shyy, W., 1998. Heat transfer enhancement with porous inserts in recirculating flows. Journal of Heat Transfer 120, 458–467.

Masuoka, T., Takatsu, Y., 1996. Turbulence model for flow through porous media. International Journal of Heat and Mass Transfer 39, 2803–2809.

Murthy, P.V.S.N., Singh, P., 1997. Effect of viscous dissipation on a non-Darcy natural convection regime. International Journal of Heat and Mass Transfer 40, 1251–1260.

Murthy, P.V.S.N., 1998. Thermal dispersion and viscous dissipation effects on non-Darcy mixed convection in a fluid saturated porous medium. Heat and Mass Transfer 33, 295–300.

Nield, D.A., 1998. Effects of local thermal non-equilibrium in steady convective processes in a saturated porous medium: forced convection in a channel. Journal of Porous Media 1, 181–186.

Peterson, G.P., Chang, C.S., 1998. Two-phase heat dissipation utilizing porous-channels of high-conductivity materials. Journal of Heat Transfer 120, 243–252.

Quintard, M., Whitaker, S., 1993. One- and two-equation models for transient diffusion processes in two-phase systems. Advances in Heat Transfer 23, 369–464.

Quintard, M., Kaviany, M., Whitaker, S., 1997. Two-medium treatment of heat transfer in porous media: numerical results for effective properties. Advances in Water Resources 20, 77–94.

Quintard, M., 1998. Modelling local non-equilibrium heat transfer in porous media. In: Heat Transfer 1998, Proceedings of the 11th International Heat Transfer Conference, vol. 1, Kyongju, Korea, pp. 279–285.

Sozen, M., Vafai, K., 1993. Longitudinal heat dispersion in porous media with real gas flow. Journal of Thermophysics and Heat Transfer 7, 153–157.

Spiga, M., Morini, G.L., 1999. Transient response of non-thermal equilibrium packed beds. International Journal of Engineering Science 37, 179–188.

Vafai, K., 1984. Convective flow and heat transfer in variable porosity media. Journal of Fluid Mechanics 147, 233–259.

Vafai, K., Kim, S., 1989. Forced convection in a channel filled with porous medium – an exact solution. Journal of Heat Transfer 111, 1103–1106.

Vafai, K., Sozen, M., 1990. Analysis of energy and momentum transport for fluid flow through a porous bed. Journal of Heat Transfer 112, 690–699.

Vafai, K., Kim, S., 1995. Discussion on forced convection in a porous channel with localized heat sources. Journal of Heat Transfer 117, 1097–1098.

Wakao, N., Kaguei, S., 1982. Heat and Mass Transfer in Packed Beds. Gordon and Breach, New York.

Yagi, S., Kunii, D., Wakao, N., 1960. Studies on axial effective thermal conductivities in porous beds. A.I.Ch.E. Journal 6, 543–546.